

Architecture of polymeric superstructures formed by locking cubic lattices of core-shell polymer microspheres

Koji Ishizu*, Takashi Ikemoto and Ayako Ichimure

Department of Polymer Science, Tokyo Institute of Technology 2-12, Ookayama, Meguro-ku, Tokyo 152, Japan

(Received 18 October 1996; revised 21 February 1997)

Poly (4-vinylpyridine) (P4VP) core-poly(α -methylstyrene) shell polymer microspheres have been synthesized by cross-linking the P4VP spherical microdomains of poly(α -methylstyrene-*b*-4-vinyl-pyridine) diblock copolymer films with 1,4-dibromobutane. These microspheres formed a lattice with a body-centred cubic structure near the overlap concentration. In the bulk of as-cast film of microspheres, this structure changed to a face-centred cubic lattice. After these microspheres formed a cubic lattice in methyl methacrylate (MMA) monomer, the polymeric superstructures were constructed by locking permanently ordered lattice in a solid matrix by means of free radical polymerization of MMA monomer. This technique is one of the best methods for creating nanoscopic polymeric superstructures composed of three phase-separated microdomains. © 1997 Elsevier Science Ltd.

(Keywords: block copolymer; core-shell microsphere; cubic lattice)

INTRODUCTION

Block and graft copolymers composed of incompatible block segments form microphase-separated structures in the solid state. We have established a novel synthesis method for core-shell microspheres: cross-linking segregated chains in spherical microdomains^{1–7}. These microspheres were stabilized even in good solvents by multiarm chains.

Such structures of core-shell microspheres are somewhat similar to those of star-shaped polymers. Dauoud and Coton⁸ were the first to study the conformations and dimensions of star polymers using the ‘thermal blob’ model. According to theoretical results⁹, the central cores of star polymers do not interpenetrate with each other even beyond the overlap threshold (C^*) in polymer solution. Thus, stars with many arms are expected to form a crystalline array near C^* .

We demonstrated previously that the core-shell microspheres led to hierarchical structure transformation of the cubic lattices^{10,11}. That is to say, these microspheres formed a lattice with a body-centred cubic (BCC) structure near C^* . In the bulk of the film, this structure changed to a face-centred cubic (FCC) lattice.

It is well known that submicron-size colloidal spheres form a BCC or FCC lattice in an aqueous solution^{12–16}. More recently, Asher *et al.*¹⁷ have developed an approach to permanently lock in the crystalline colloidal array ordering in a solid matrix. They introduced into the crystalline colloidal array highly purified non-ionic polymerizable monomers that can form a network around the spherical particles. We have also constructed polymeric superstructures by free radical polymerization of N-vinylpyrrolidone (VP) monomer as a matrix, after polypyrrole microspheres were arranged to an BCC lattice in VP monomer solution¹⁸.

In this article, we report the architecture of polymeric superstructure films formed by locking the cubic lattices of core-shell microspheres in a poly(methyl methacrylate) (PMMA) matrix. Poly(4-vinylpyridine) (P4VP) core-poly(α -methylstyrene) (PMS) shell microspheres were synthesized by cross-linking the P4VP spherical microdomains of poly[α -methylstyrene (MS)-*b*-4-vinylpyridine (4VP)] diblock copolymer films with a 1,4-dibromobutane (DBB). These microspheres formed the lattice with a BCC structure near C^* . In the bulk of the film, this structure changed to an FCC lattice. After these microspheres formed a cubic lattice in methyl methacrylate (MMA) monomer, the polymeric superstructures were constructed by locking permanently ordered lattice in a solid matrix by means of free radical polymerization of MMA. The microstructures of such periodic materials were studied by small-angle X-ray scattering (SAXS), transmission electron microscopy (TEM) and thermal analysis.

EXPERIMENTAL

Synthesis and characterization of core-shell microspheres

The well-defined poly (MS-*b*-4VP) diblock copolymer (MSV1) was prepared by the sequential anionic polymerization using *n*-butyllithium as an initiator in tetrahydrofuran (THF) at 1–78°C. The details concerning the synthesis, purification and characterization of diblock copolymers have been given elsewhere¹. The morphological structure of MSV1 specimen cast from toluene showed P4VP spheres in a PMS matrix. Table 1 lists the characteristics of poly (MS-*b*-4VP) diblock copolymer MSV1.

Core-shell polymer microspheres were synthesized by cross-linking the segregated chains in P4VP spherical microdomains with 1,4-dibromobutane (DBB) vapour at room temperature. The details concerning the synthesis and the characterization of such microspheres have been given previously¹⁹.

* To whom correspondence should be addressed

Table 1 Characteristics of poly (MS-b-4VP) diblock copolymer

Code	Diblock copolymer $10^{-4} \cdot \bar{M}_n^a$ (g mol ⁻¹)	\bar{M}_w/\bar{M}_n^b	Content of P4VP block ^c (mol%)	Domain size ^d \bar{D}_n	\bar{D}_w/\bar{D}_n
MSV1	6.0	1.17	22	16.0	1.01

^aDetermined by osmometry.

^bDetermined by gel permeation chromatograph.

^cDetermined by ¹H-n.m.r.

^d \bar{D}_n indicates the diameter of P4VP spheres and was determined by TEM micrographs cast from toluene. Size distribution (\bar{D}_w/\bar{D}_n) estimated from TEM micrographs.

Morphological observation

Ultrathin film specimen of the starting diblock copolymer was prepared for the transmission electron microscopy (TEM) observations by placing a drop of a 1 wt% toluene solution on a microscope mesh coated with a carbon film, and then evaporating the solvent as slowly as possible at 25°C. This specimen was exposed to osmium tetroxide (OsO₄) vapour for 24 h at room temperature.

For two-dimensional observation of the packing structure of the microsphere in bulk, an ultrathin film 80 nm thick was prepared by cutting with a microtome (Reinhert-Nissei Co., Ultracut N) and stained with OsO₄. Morphological results were obtained on a JEOL 100CX TEM at 100 kV.

Measurements of dynamic light scattering

The hydrodynamic diameter (\bar{D}_h) of core-shell microspheres was determined using a dynamic light scattering (DLS; scattering angle = 90°, Otsuka Electric Co., Photal TELS-6000HL) in 0.01 wt% benzene ($\eta = 0.654$ cp, $n_D = 1.501$) solution at 25°C.

SAXS measurements

The SAXS intensity profile was measured with a rotating-anode X-ray generator (Rigaku Denki Rotaflex RTP 300RC) operated at 40 kV and 100 mA. The X-ray source was monochromatized to Cu K α ($\lambda = 1.5418$ Å) radiation. In the measurement of the sample solutions, we used a glass capillary ($\phi = 2.0$ mm, Mark-Röhrchen Ltd.) as a holder vessel.

Locking of superlattice

The locking of the superlattice was carried out by following three methods. (1) The prescribed MMA solution of core-shell microspheres was poured into a petri dish. Photopolymerization of MMA was carried out in the presence of 2,2'-azobisisobutyronitrile (AIBN; 2 wt% for monomer) and benzoin methyl ether (1 wt% for monomer) as a photosensitizer under the irradiation with a u.v. beam in a nitrogen atmosphere at 20°C for 5 h (250 W high-pressure mercury lamp, Ushio Denki UI 250D; irradiation distance 30 cm). (2) The prescribed MMA solution of core-shell microspheres was poured into the sample bottle with a stopper. Free radical polymerization of MMA was carried out in the presence of 2,2'-azobis (4-methoxy-2,4-dimethylvaleronitrile) (V-70; Wako Pure Chemical Ind. Ltd., 2 wt% for monomer) and tetrabromomethane (CBr₄; 2 wt% for monomer) under a nitrogen atmosphere at 40°C for 10 h. (3) Similar radical polymerization containing not only V-70 and CBr₄, but also ethylene glycol dimethacrylate (EGDM; 3 wt% for monomer) as a cross-linking reagent was carried out in the same polymerization condition. After polymerization, the SAXS measurements were taken for such films formed in order to check the locking of microsphere lattices.

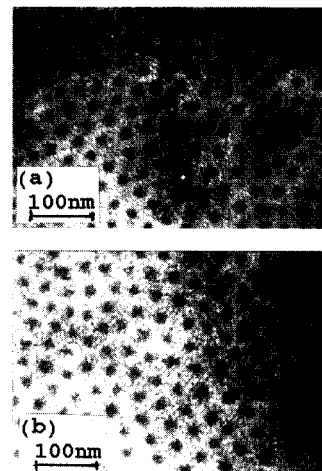


Figure 1 TEM micrographs of diblock copolymer specimen MSV1 (a) and core-shell microsphere MSV1-M (b) cast from toluene.

Thermal analysis

Differential scanning calorimetry (DSC) measurements were recorded on a Seiko Instruments DSC 220C to determine glass transition temperatures (T_g). Indium and zinc were used as calibration standards. Heating rate was 120°C min⁻¹.

RESULTS AND DISCUSSION

Synthesis of core-shell polymer microspheres

Figure 1(a) shows typical TEM micrograph of MSV1 diblock copolymer specimen cast from toluene. The dark portions are the selectively stained P4VP blocks. This specimen shows the texture of dispersed P4VP spheres in a PMS matrix. The absolute value of the diameter ($\bar{D}_n = 16.0$ nm) of the P4VP spheres is listed in Table 1. The \bar{D}_w/\bar{D}_n size distribution (where \bar{D}_w is the weight-average diameter) is very narrow for this specimen. It was mentioned previously from SAXS measurements that P4VP spherical microdomains were packed with a BCC arrangement¹⁹.

The segregated spherical P4VP domains were cross-linked using DBB vapour in the solid state. The cross-linked product (MSV1-M) freely dissolved in organic solvents such as benzene, toluene, THF and chloroform. In order to estimate the core size of the cross-linked products, TEM observations of the cross-linked products which had been stained with OsO₄, were carried out.

Figure 1(b) shows typical TEM micrograph of MSV1-M cast from 1.0 wt% toluene solution. This specimen corresponds to the restructural film from core-shell microspheres. It is found from this micrograph that P4VP cores (dark

Table 2 Characteristics of core-shell microsphere

Code	\bar{R}_c^a (nm)	$10^{-6} \cdot \bar{M}_w^b$ (g mol ⁻¹)	f^c	\bar{D}_h^d (nm)	C^*^e (wt%)
MSV1-M	8.1	6.94	116	50.9	8.73

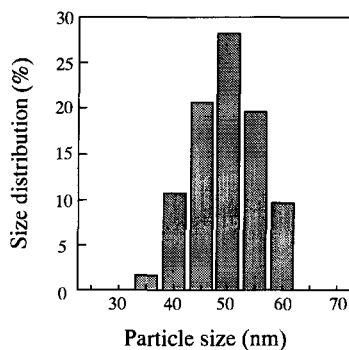
^aRadius of P4VP cores determined by TEM micrographs.

^bTotal molecular weight of microsphere determined by static light scattering (SLS).

^cArm number (aggregation number of block copolymers), estimated from \bar{M}_w of microsphere and \bar{M}_n of arm block.

^dDetermined by DLS in benzene.

^eOverlap threshold in benzene solution calculated from the \bar{D}_h values in benzene.

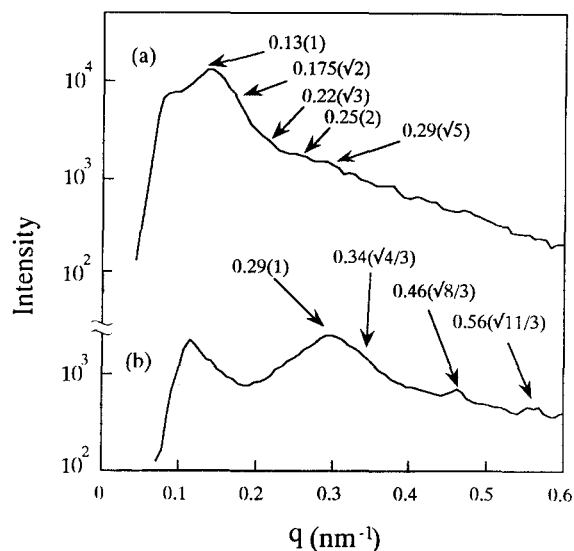
**Figure 2** Particle size distribution of microsphere MSV1-M.

portions, the average radius $\bar{R}_c = 8.1$ nm) with a narrow size distribution are dispersed in a PMS matrix. The core size of P4VP domains is almost the same as that of MSV1 film (diameter of P4VP spheres $\bar{D}_n = 16.0$ nm; see in Table 1) even if after cross-linking treatment. Moreover, P4VP cores seem to arrange in some kinds of ordered structures. Such ordering of microspheres will be discussed in the section of SAXS measurements. The arm number (aggregation number of block copolymers: f) was estimated from the total molecular weight (\bar{M}_w) of microspheres and \bar{M}_n of arm block. These characteristics of the MSV1-M microsphere are listed in Table 2.

The hydrodynamic diameter (\bar{D}_h) of microspheres was determined in benzene by means of DLS. Figure 2 shows the result of particle size distribution for the MSV1-M microsphere. It is found that the MSV1-M microsphere has a narrow particle size distribution and the average particle size is 50.9 nm. The overlap thresholds in polymer solutions (C^*)²⁰ of the MSV1-M microsphere in benzene was calculated to be 8.73 wt% from the \bar{D}_h and the total molecular weight of the microsphere. These characteristics are also listed in Table 2.

Ordering of core-shell microsphere in MMA solutions

Below the C^* , the microspheres remain isolated, as any ordered arrangements of microspheres in MMA monomer are expected to appear near or above the C^* . So, we studied the possibility of structural ordering of microspheres in MMA monomer by means of SAXS and TEM measurements, varying the microsphere concentrations with reference to the C^* values in benzene. Figure 3 shows typical SAXS intensity profiles for the MMA solutions of MSV1-M microsphere (12 and 100 wt% microsphere concentrations) in the small-angle region, where $q [= (4\pi/\lambda)\sin\theta]$ is the magnitude of the scattering vector. The values shown in Figure 3 indicate the q . The arrows show the scattering maxima and the values in the parentheses indicate the interplanar spacings (d_1/d_i) calculated from Bragg reflections. Below 7 wt% MMA monomer solution, no regular scattering peaks appeared due to disordering. At 12 wt%

**Figure 3** SAXS intensity profiles for MMA solutions of microsphere MSV1-M: (a) 12 wt% microsphere concentration; (b) 100 wt% microsphere concentration (bulk film).

microsphere concentration ($C^* = 8.7$ wt%), the first five peaks appear closely at the relative q positions of 1: $\sqrt{2}$: $\sqrt{3}$: 2: $\sqrt{5}$ as shown in parentheses. The interplanar spacing (d_1/d_i) at the scattering angles is relative to the angle of the first maximum according to Bragg's equation: $2d \sin\theta = n\lambda$ (where θ is one-half the scattering angle, $\lambda = 1.5418$ Å). In general, this packing pattern appears in the lattice of not only simple cubic, but also BCC structures. As mentioned in Section 1, core-shell microspheres were packed in the lattice of a BCC structure near C^* .^{10,11} Therefore, these values correspond to packing pattern of (110), (200), (211), (220) and (310) planes in a BCC structure. It is therefore concluded that the core-shell microspheres are packed in the lattice of a BCC structure near C^* .

In the bulk film (100 wt% microsphere concentration), the first four peaks appear closely at the relative q positions of 1: $\sqrt{4/3}$: $\sqrt{8/3}$: $\sqrt{11/3}$ as shown in parentheses. On the other hand, the TEM micrograph of the bulk film specimen is shown in Figure 1(b). Dark P4VP cores are regularly packed with long-range order. It is therefore concluded that the microspheres are packed in the lattice of a FCC structure in the bulk film. This is the most efficient way to pack spheres. Moreover, the core radius of P4VP can be also estimated from the SAXS data. The Bragg spacing d_1 for the (111) plane on a FCC structure is estimated to be 21.5 nm from the first scattering peak ($q = 0.29$ nm⁻¹, $2\theta = 0.41^\circ$). d_1 is related to the cell edge a_c of the cubic lattice as follows:

$$a_c = \sqrt{3}d_1 \quad (1)$$

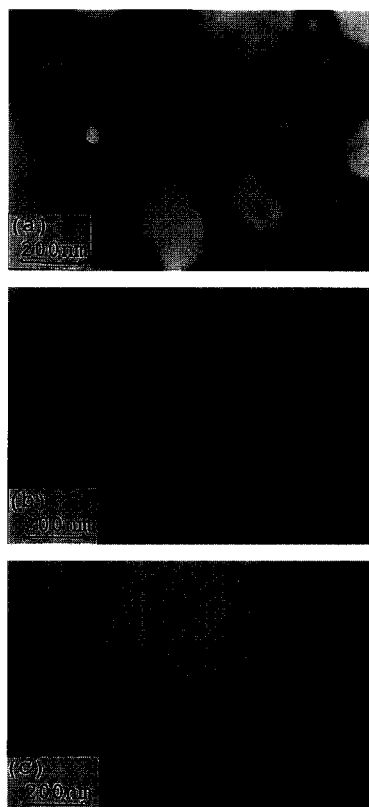


Figure 4 TEM micrographs of film specimens after locking treatments: (a) locking by Method 1; (b) locking by Method 2; (c) locking by Method 3.

and

$$R_c = (3v/16\pi)^{1/3} a_c \quad (2)$$

where v is the volume fraction of the core.

Assuming that $v = 0.2$, R_c is calculated to be 8.5 nm from equations (1) and (2). This value is in good agreement with the one (8.1 nm) observed from the TEM micrograph. Thus, the core-shell microspheres led to hierarchical structure transformation of the cubic lattices with increasing the polymer concentration. Hence, such polymeric superstructures can be expected to form by locking permanently ordered lattice in a solid matrix by means of free radical polymerization of MMA.

Locking of superlattice

At first, the photopolymerization of 12 wt% MMA solution of MSV1-M microsphere containing AIBN and benzoin methyl ether was carried out under u.v. irradiation (Method 1). *Figure 4(a)* shows the TEM micrograph of the film specimen after locking treatment. Dark portions correspond to P4VP cores. On the other hand, white portions correspond to PMMA or PMS shell parts. Large white domains appear at places in this micrograph independently of gathering parts of core-shell microspheres. It is reasonable to judge that these macrodomains correspond to PMMA phases. This polymerization system seemed to lead polymerization-induced phase separation. Moreover, PMS chains on shell part were degraded by u.v. irradiation (this fact was recognized from viscometric measurement of MSV1-M film before and after u.v. irradiation).

Next, free radical polymerization of 12 wt% MMA solution of MSV1-M microsphere containing V-70 and

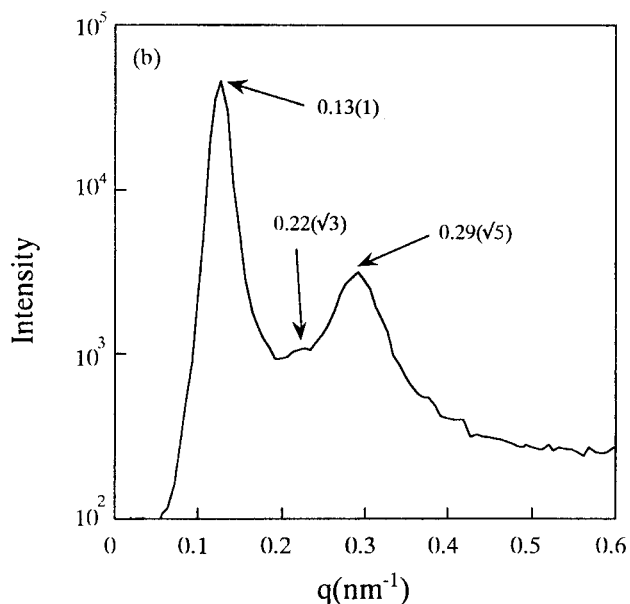
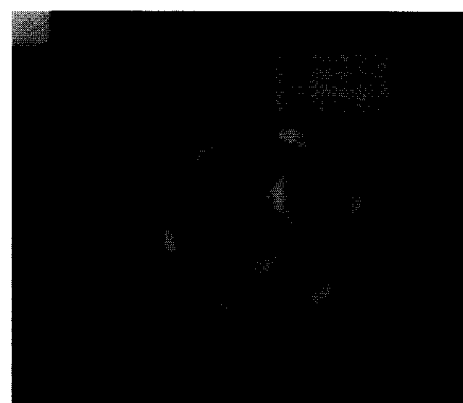


Figure 5 SAXS pattern and its intensity profile for MSV1-M-LA film: (a) SAXS pattern image; (b) SAXS intensity profile.

CBr_4 was carried out in a sealed sample bottle (Method 2). Addition of CBr_4 as a chain transfer reagent can be expected to shorten the propagating chain length of MMA with the intention of preventing the polymerization-induced macrophase separation. We obtained a transparent film by such procedure. *Figure 4(b)* shows the TEM micrograph of the film specimen after locking treatment. The MMA monomers form a continuous matrix phase around the lattice of core-shell microspheres by polymerization. However, the microspheres are not maintained perfectly with a BCC packing, but are packed with irregular arrangement at places.

Subsequently, free radical polymerization of 12 wt% MMA solution of MSV1-M microsphere containing V-70, CBr_4 and EGDM was carried out in the same conditions as Method 2 (Method 3). We also obtained a transparent film following this procedure. *Figure 4(c)* shows the TEM micrograph of the film specimen after locking treatment (MSV1-M-LA) by means of Method 3. It is indicated from this texture that P4VP cores are packed hexagonally in a two-dimensional aspect. *Figure 5(a)* and (b) show the SAXS pattern and its intensity profile of the solid film MSV1-M-LA, respectively. In this profile, the first three peaks appear at the relative q positions of $1 : \sqrt{3} : \sqrt{5}$ as shown in parentheses. This packing pattern is identical to the interplanar spacings of a BCC structure. It is therefore

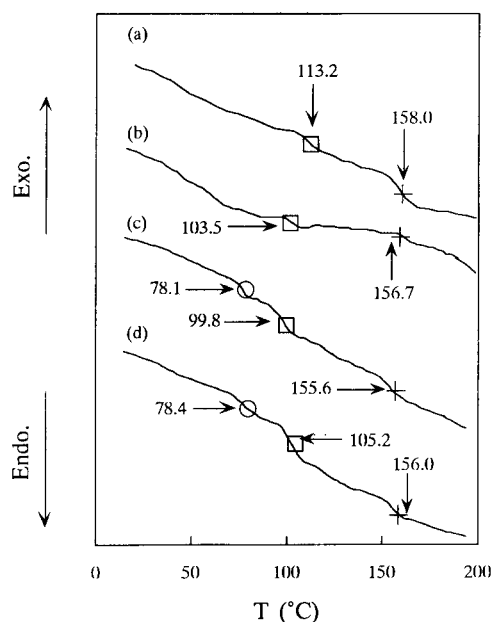


Figure 6 DSC thermograms of polymer films: (a) diblock copolymer MSV1; (b) core-shell microsphere MSV-M; (c) binary blend of MSV1-M and PMMA; (d) polymeric superstructure MSV1-M-LA.

concluded that the MSV1-M microspheres were locked with a BCC lattice in PMMA network by free radical polymerization. Addition of chain transfer and cross-linking reagents was very effective in preventing the polymerization-induced macrophase separation of PMMA. It is also noticed that the first peak ($q = 0.13 \text{ nm}^{-1}$, $2\theta = 0.18^\circ$) of the MSV1-M-LA is identical to the q positions of an MMA solution of microsphere (MSV1-M-LB; 12 wt% microsphere concentration). This fact means that the volume shrinkage of PMMA has never occurred during free radical polymerization. Judging from the densities of MMA (0.936 g cm^{-3}) and PMMA (1.88 g cm^{-3})²¹, the volume shrinkage of PMMA is estimated to be 21.2 vol% after locking treatment. Then, the domain spacing of nearest-neighbour microspheres should decrease by 8% in length compared to that of MSV1-M-LB. We could not obtain the good accuracy concerning the volume shrinkage of PMMA in this experiment.

Space arrangement of polymeric superstructures

In a solid film, it is important to make clear whether PMS arm chains in the shell part are miscible or immiscible to PMMA matrix chains during free radical polymerization. DSC measurement of the solid films is one of the best methods to resolve such problem. The DSC thermograms of diblock copolymer MSV1 (a), core-shell microsphere MSV1-M (b), binary blend of MSV1-M/PMMA (2/13 wt/wt) (c), and polymeric superstructure MSV1-M-LA (d) are presented in Figure 6. Two glass transition temperatures (T_g) are clearly visible in the traces of both MSV1 (a) and MSV1-M (b). These transition points correspond to the

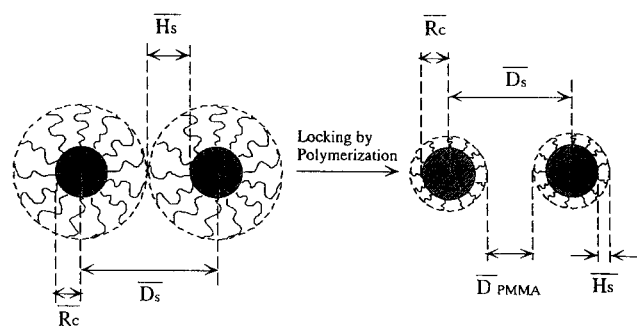


Figure 7 Illustration of space arrangement for the nearest-neighbor core-shell microspheres before and after locking.

P4VP block or cross-linked P4VP core in the range 100–110°C and the PMS block at temperatures above 156°C. The T_g of hydrophobic P4VP block is somewhat higher than that of hydrophilic cross-linked P4VP core. The existence of block-specific glass transition temperatures is indicative of phase demixing and therefore constitutes a fingerprint of microphase separation. In the DSC trace of MSV1-M-LA (d), three endothermic peaks appear at temperatures of 78, 105 and 156°C. A similar result is obtained in the DSC trace of binary blend of MSV1-M/PMMA [Figure 6(c)]. Then, the T_g of PMMA corresponds to 78°C. It is concluded that the polymeric superstructure prepared by locking is composed of three phase-separated microdomains, i.e. P4VP cross-linked core, PMS shell and PMMA matrix.

We consider the space arrangement of the cubic lattice in polymeric superstructures. The measured Bragg spacing d_1 is related to the cell edge a_c of the cubic lattice and the nearest-neighbour distance (D_s) of the spheres as follows:

$$D_s = (\sqrt{3}/2)a_c = (\sqrt{3}/2)d_1 \text{ for BCC} \quad (3)$$

$$D_s = (1/\sqrt{2})a_c = (\sqrt{3}/2)d_1 \text{ for FCC} \quad (4)$$

Figure 7 shows the illustration of the space arrangement for the nearest-neighbour core-shell microspheres before and after locking. Where \bar{H}_s and \bar{D}_{PMMA} are the thickness of shell part and the distance of PMMA matrix between nearest-neighbour microspheres. The stretched PMS arm chains stabilized sterically the P4VP cross-linked cores in MMA solution. After locking of superlattice of microspheres, the PMS arm chains (shell thickness $\bar{H}_s = 4.7 \text{ nm}$) cover around the surface of P4VP cross-linked core ($\bar{R}_c = 8.5 \text{ nm}$, employed from SAXS data) due to immiscibility between PMS and PMMA chains. Where the value of \bar{H}_s was evaluated from the SAXS data (FCC lattice) of microsphere MSV1-M in the bulk film. Table 3 lists the domain spacings of nearest-neighbour microspheres before and after locking. The observed value of \bar{D}_{PMMA} is 33.6 nm. Considering the effect of the volume shrinkage of PMMA matrix, the \bar{D}_{PMMA} value is speculated to be 30.9 nm. Further investigation concerning the volume shrinkage is necessary.

Table 3 Domain spacings of nearest-neighbour microspheres before and after locking

Code	State	\bar{D}_s (nm)	\bar{R}_c (nm)	\bar{H}_s (nm)	\bar{D}_{PMMA}
MSV1-M-LB	MMA solution	60.0	8.5	21.5	—
MSV1-M-LA	Solid film	60.0	8.5	4.7	33.6

^aDetermined by SAXS data on FCC lattice of MSV1-M film.

The interplaner spacings of superstructures can be controlled by changing the monomer concentration and type of cubic lattices. The work here demonstrates a method for preparing polymeric superstructures composed of nanoscopic cubic lattices. These systems will have numerous applications in technology such as optical materials. Results of such investigations will be reported in the near future.

ACKNOWLEDGEMENTS

This work was supported in part by a Grant in Aid for Scientific Research (Priority Areas of 'New Polymers and Their Nano-Organized Systems' (no. 277/08246218) from the Ministry of Education, Science, Sports and Cultures, Japan.

REFERENCES

1. Ishizu, K. and Fukutomi, T., *Journal of Polymer Science. Polymer Letters Edition*, 1988, **26**, 281.
2. Ishizu, K., *Polymer*, 1989, **30**, 793.
3. Ishizu, K., *Polymer Communications*, 1989, **30**, 209.
4. Ishizu, K. and Onen, A., *Journal of Polymer Science. Polymers Chemistry Edition*, 1989, **27**, 3721.
5. Saito, R., Kotsubo, H. and Ishizu, K., *European Polymer Journal*, 1991, **27**, 1153.
6. Saito, R., Kotsubo, H. and Ishizu, K., *Polymer*, 1992, **33**, 1073.
7. Ishizu, K. and Saito, R., *Polymer Plastic Technology Engineering*, 1992, **31**, 607.
8. Daoud, M. and Cotton, J.P., *Journal of Physics (Les Ulis)*, 1982, **43**, 531.
9. Witten, T.A., Pincus, P.A. and Cates, M., *Europhysics Letters*, 1986, **2**, 137.
10. Ishizu, K., Sugita, M., Kotsubo, H. and Saito, R., *Journal of Colloid Interface Science*, 1955, **169**, 456.
11. Ishizu, K., *Macromolecule Reports*, 1995, **A32**, 759.
12. Kesavamoorthy, R., Tandon, S., Xu, S., Jagannathan, S. and Asher, S.A., *Journal of Colloid Interface Science*, 1992, **153**, 188.
13. Aastuen, D.J.W., Clark, N.A., Cotter, L.K. and Ackerson, B., *Physics Review Letters*, 1986, **57**, 1733.
14. Hiltner, P.A., Papir, Y.S. and Krieger, I.M., *Journal of Physics and Chemistry*, 1881, **1971**, 75.
15. Monovoukas, Y. and Gast, A.P., *Journal of Colloid Interface Science*, 1989, **128**, 333.
16. Kose, A., Osaki, T., Kobayashi, Y., Takano, K. and Hachisu, S., *Journal of Colloid Interface Science*, 1973, **44**, 330.
17. Asher, S.A., Holtz, J., Liu, L. and Wu, Z., *Journal of the American Chemistry Society*, 1994, **116**, 4997.
18. Ishizu, K. and Honda, K., *Polymer*, 1997, **38**, 689.
19. Ishizu, K., *Journal of Colloid Interface Science*, 1993, **156**, 299.
20. Glassley, W.W., *Advances in Polymer Science*, 1974, **16**, 1.
21. Gall, W.G. and McCrum, N.G., *Journal of Polymer Science*, 1961, **50**, 489.